European Journal of Pharmaceutical Sciences 65 (2014) 79–88

Contents lists available at ScienceDirect

European Journal of Pharmaceutical Sciences

journal homepage: www.elsevier.com/locate/ejps

Technetium-99m-labeled nanofibrillar cellulose hydrogel for *in vivo* drug release

Patrick Laurén [a,*], Yan-Ru Lou [a], Mari Raki [b], Arto Urtti [b], Kim Bergström [b], Marjo Yliperttula [a]

[a] Division of Pharmaceutical Biosciences, Faculty of Pharmacy, P.O. Box 56, FI-00014 University of Helsinki, Finland
[b] Centre for Drug Research, Faculty of Pharmacy, P.O. Box 56, FI-00014 University of Helsinki, Finland

ARTICLE INFO

Article history:
Received 8 March 2014
Received in revised form 14 July 2014
Accepted 11 September 2014
Available online 20 September 2014

Keywords:
Nanofibrillar cellulose
Hydrogel
SPECT/CT
Technetium-99m
Drug release
Delivery

ABSTRACT

Nanoscale celluloses have recently gained an increasing interest in modern medicine. In this study, we investigated the properties of plant derived nanofibrillar cellulose (NFC) as an injectable drug releasing hydrogel *in vivo*. We demonstrated a reliable and efficient method of technetium-99m-NFC labeling, which enables us to trace the *in vivo* localization of the hydrogel. The release and distribution of study compounds from the NFC hydrogel after subcutaneous injection in the pelvic region of BALB/c mice were examined with a multimodality imaging device SPECT/CT. The drug release profiles were simulated by 1-compartmental models of Phoenix® WinNonlin®. The NFC hydrogel remained intact at the injection site during the study. The study compounds are more concentrated at the injection site when administered with the NFC hydrogel compared with saline solutions. In addition, the NFC hydrogel reduced the elimination rate of a large compound, technetium-99m-labeled human serum albumin by 2 folds, but did not alter the release rate of a small compound ^{123}I-β-CIT (a cocaine analogue). In conclusion, the NFC hydrogels is easily prepared and readily injected, and it has potential use as a matrix for controlled release or local delivery of large compounds. The interactions between NFC and specific therapeutic compounds are possible and should be investigated further.

1. Introduction

The use of hydrogels as nanostructured scaffolds and particles in tissue engineering and delivery of therapeutic agents is an emerging field in biomedicine (Geckil et al., 2010; Lu et al., 2013), as many hydrogels have innate structural similarities with physiological matrices (Slaughter et al., 2009). However, there is an ongoing research to improve the properties and quality of these applications, such as structural integrity, biocompatibility, and biodegradability. Recently, cellulose and cellulose-based materials have gained an increasing interest in modern medicine, mostly due to their versatility and inherent properties (Charreau et al., 2013).

Cellulose is the most abundant naturally occurring biopolymer on earth. The discovered structural features and properties have enabled the creation of novel cellulose-based materials and applications, particularly the emerging investigation of nanoscale celluloses (Charreau et al., 2013). The cellulose nanomaterials, mostly films and hydrogels, have already shown importance in industrial, pharmaceutical, and biomedical research (Klemm et al., 2011). In the biomedical field, injectable hydrogels have shown some potential (Jain et al., 2013); especially considering the challenges of non-invasive delivery of peptide and protein therapeutics, such as monoclonal antibodies and recombinant human proteins (Jain et al., 2013; Kumar et al., 2006; Muller and Keck, 2004).

Modern medicine involving drug delivery and therapy with implants and hydrogels, the applications must be non-toxic and biocompatible, while still providing the desired properties and functions for successful treatment. Currently, the modern medicine related research on nanostructural cellulose hydrogels has mostly focused on the use of bacterial celluloses (Innala et al., 2013; Muller et al., 2013; Pretzel et al., 2013). However, plant-derived nanofibrillar cellulose (NFC) prepared from wood pulp is also one of the emerging nanomaterials with properties for potential biomedical applications (Bhattacharya et al., 2012). High water content of NFC, like with many hydrogels, provides soft tissue like mechanical behavior and similarity, which inherently improves biocompatibility (Jain et al., 2013). Furthermore the viscoelastic properties of NFC resemble the physiological properties of extracellular matrices (Bhattacharya et al., 2012; Miron-Mendoza et al., 2010). The NFC aqueous suspensions behave as 1-compartmental hydrogels with pseudoplastic and thixotropic properties (Pääkkö et al., 2007). Pseudoplasticity induces a shear thinning

* Corresponding author. Tel.: +358 5 05124191.
E-mail address: patrick.lauren@helsinki.fi (P. Laurén).

http://dx.doi.org/10.1016/j.ejps.2014.09.013
0928-0987/

effect which reduces viscosity with increased shear stress. Shear thinning therefore enables NFC hydrogels to be easily injected (Bhattacharya et al., 2012) as the extruding force of the syringe is enough to change NFC flow properties to lower the viscosity. While in static conditions, NFC retains higher viscosity due to the rearrangement of the fibers, which reverts the shear thinning effect. As an injectable hydrogel, NFC is able to deliver cells or therapeutic agents (e.g. proteins or peptides) into easily accessible target sites, such as under the skin. Additionally NFC hydrogels are biocompatible, non-toxic, and structurally durable (Märtson et al., 1999; Vartiainen et al., 2011). As a plant derived material, the NFC hydrogels are obtained from a non-animal and non-human source, being thus xeno-free. Additionally, cellulose based materials offer a broad modification capacity (Klemm et al., 2011), which is advantageous when designing new biomaterials.

Currently, in biomedical and -pharmaceutical research, the hydrogels under investigation for the potential use of controlled release matrices can prove to be problematic in terms of gel activation properties (Hennink and van Nostrum, 2002), especially with injectable hydrogels. The need for an external source of activation presents additional complications and toxicity as crosslinking agents often used are potentially toxic compounds (Van Tomme et al., 2008), that need to be extracted from the gels before usage. This could prove to be difficult in the case of parenteral delivery, such as subcutaneous injections. Furthermore, the crosslinkers may react with the imbedded drug compounds within the hydrogel, which may result to unwanted consequences or ineffective treatment. NFC overcomes this obstacle, as there is no need for activation methods such as the use of UV irradiation or chemical crosslinking due to the pseudoplasticity of the material. After administration (e.g. subcutaneous injection), NFC "gels" spontaneously, as the fibers rearrange to form a viscous gel; therefore avoiding all the complications with removing the crosslinking agents, potential toxicity or interactions between the crosslinking agents and the drug compounds in use.

The aim of this study was to investigate the properties of plant-derived NFC hydrogel as an injectable platform or "implant" for drug release, in addition to examine the utility of SPECT/CT imaging to illustrate the behavior of hydrogels *in vivo*. We investigated the use of NFC hydrogel as a potential device for local delivery and/or sustained drug release in an *in vivo* study with the use of BALB/c inbred mice. Furthermore the use of radiolabeled wood pulp NFC hydrogel as a potential biomedical device amongst other biomedical applications has not been demonstrated before. However, the biocompatibility and toxicity of bacterial and plant-derived cellulose materials have been documented both in vitro and *in vivo* use with of small animals (Märtson et al., 1999; Vartiainen et al., 2011; Alexandrescu et al., 2013; Roman et al., 2010; Kovacs et al., 2010; Pértile et al., 2011; Helenius et al., 2006; Moreira et al., 2009). In addition, we demonstrate a reliable and efficient method for NFC radiolabeling for the purpose of molecular imaging with a small animal SPECT/CT.

2. Materials and methods

2.1. ^{99m}Tc-NFC labeling

To image NFC in animals by SPECT/CT, NFC was labeled with ^{99m}Tc-NFC according to a previously described procedure for ^{99m}Tc-labeled carboxymethyl-cellulose (Schade et al., 1991) with slight modifications. 1.6% NFC stock hydrogel (GrowDex®, UPM-Kymmene Corporation, Finland) was used to prepare 1% NFC hydrogel with added stannous chloride stock (17.5 μg/ml in saline solution) and ^{99m}Tc-pertechnetate ($^{99m}TcO_4^-$) stock (~80 MBq/ml in saline solution) to a final volume of 1 ml. Briefly, 590 μl of the stock NFC was added to 285 μl of stannous chloride dehydrate solution (Angiocis®, IBA Molecular, Belgium) followed with 10 min incubation and mixing. Subsequently, 125 μl of $^{99m}TcO_4^-$ was added to the reaction mixture to reach the NFC concentration of 1% and incubated while mixing for 30 min.

To optimize the method for ^{99m}Tc-NFC labeling, various conditions were tested during the labeling procedure, such as buffer pH ranging from 4.74 to 8.05, different incubation times for $^{99m}TcO_4^-$/NFC reaction mixture (5, 10, 15, 20, 25 and 30 min) and stannous chloride concentrations ranging from 50 to 0.05 μg/ml.

The stability of the radiolabel was investigated in neutral isotonic pH by incubating the 1% ^{99m}Tc-NFC samples for 24 h. Samples were prepared in stock solutions as described above in saline or in fetal bovine serum (FBS) (Sigma–Aldrich, Finland). Radiochemical purity and efficiency was tested at every time point (0, 15, 60, 120, 240 min and 24 h).

TLC determined labeling efficiency and radiochemical purity of ^{99m}Tc-NFC with ITLC-SG chromatography plates (Agilent Technologies, Santa Clara, CA, USA) in methylethylketone (MEK) solvent system. Plates were cut in smaller equally sized pieces and placed in standard RIA tubes for radioactive measurement with a gamma counter (RiaCalc. WIZ, Wallac 1480 WIZARD® 3″, Finland).

2.2. In vivo imaging, drug release and kinetics

Animal studies were approved by the Finnish National Animal Experiment Board and performed in accordance with the Animal Welfare Act (247/1996) and Good Laboratory Practices for Animal Research. The release properties of plant-derived NFC implants were investigated with the use of radiolabeled small compounds. The use of ^{99m}Tc-NFC allows localization of the NFC in animals. Hydrogel implants were injected subcutaneously in the pelvic region, and the mice were observed non-invasively over a 24 h period with the use of a SPECT/CT system. After the 24 h period, the mice were sacrificed by cervical dislocation.

A total of 20 female BALB/c inbred mice were obtained from a professional stockbreeder (Harlan Laboratories, Netherlands) and quarantined for two weeks prior to the start of the experiment. The mice were divided into 7 groups, A, B, C, D, E, F ($n = 3$) and G ($n = 2$). The mice in groups A and C were injected with a mixture of saline solution and Iodine-123-Sodium Iodine (^{123}I-NaI) or with a cocaine analogue Iodine-123-(2-beta-carbomethoxy-3-beta-(4-iodophenyl)-tropane) (^{123}I-β-CIT) (MAP Medical Technologies Oy, Finland), respectively. The mice in groups B and D were injected with a 5:1 mixture of 1% NFC and ^{123}I-NaI or ^{123}I-β-CIT, respectively (final mixture of 0.83% NFC hydrogel with added study compound). Group E was injected with a mixture of ^{123}I-NaI and ^{99m}Tc-NFC for dual-radionuclide SPECT/CT. Groups F and G were injected similarly with 5:1 mixture of 1% NFC and ^{99m}Tc-labeled human serum albumin (HSA) (Sigma–Aldrich, Finland) or ^{99m}Tc-labeled HSA in a saline solution, respectively (final mixture of 0.83% NFC hydrogel with added study compound). All mice received 50–60 MBq/200 μl injections.

^{99m}Tc-HSA was prepared, and radiochemical purity was tested according to the manufacturer's instructions (Vasculocis®, CIS bio international, France). Radiochemical impurities were found below the allowed 5% of the total activity.

SPECT/CT imaging was performed with a four-headed small animal scanner (NanoSPECT/CT®, Bioscan, USA), outfitted with 1.0 mm multipinhole apertures. All mice were sedated with isoflurane, and SPECT images were acquired 0 h (with 5 or 6 acquisitions at 15 min intervals), 5 h and 24 h post-injection in 16 projections using time per projection of 45, 90 and 180 s, respectively. CT imaging was accomplished with 45 kVp tube voltage in 180 projections. For 3D co-registration and analysis, the SPECT images were reconstructed with HiSPECT NG software (Scivis GmbH, Germany) and fused with CT datasets by using the molecular imaging suite

InVivoScope™ (Bioscan Inc., USA). In the analysis, volumes of interests (VOI's) were drawn at the injection site (whole NFC implant), thyroid glands, stomach, left kidney, heart, and around the striatum depending on the study compound, respectively. Counts within each VOI were recorded, corrected for radioactive decay, and normalized to the activity at the time of injection.

^{99m}Tc-HSA release kinetics was described using the built-in 1-compartmental models of Phoenix® WinNonlin® (Pharsight, Mountain View, USA). The saline preparations were assumed to be 100% available for absorption immediately after injection. The pharmacokinetic (PK) data obtained from the saline injections were observed against the data obtained from the hydrogels. Deconvolution and Loo–Riegelman models were selected to demonstrate ^{99m}Tc-HSA release, or the amount ready to be absorbed, from the injected hydrogel.

3. Results

3.1. ^{99m}Tc-NFC labeling

^{99m}Tc was chosen to label NFC based on the previous finding showing the binding of ^{99m}Tc to carboxymethyl-cellulose (Schade et al., 1991). To optimize the labeling condition, we investigated the following parameters: the concentration of stannous chloride solution required for the reduction of ^{99m}Tc (Fig. 1a), the pH of the labeling solution (Fig. 1b), and the time required for the labeling reaction to occur efficiently (data not shown). Stannous chloride at 5 μg/ml is shown to be the most optimal; however, the labeling procedure was fairly insensitive towards the concentration changes, and no major effect on labeling efficiency was found between the concentrations of 50 and 0.5 μg/ml (Fig. 1a). For further studies, the optimal 5 μg/ml stannous chloride concentration was selected. In addition, the changes of pH in the labeling solutions were investigated during the radiolabel preparation. It was observed that the tested pH levels did not have any noticeable effect on the labeling efficiency (Fig. 1b). Throughout the pH range of 4.74–8.05, the labeling efficiency was found well over 95%. The saline solution (pH of 7.2) was selected for animal studies. Furthermore the incubation times before the TLC radiolabel purity confirmation were examined. It was shown that the incubation times less than 30 min were suboptimal (data not shown). Therefore 30 min incubation time was selected for further studies.

The described ^{99m}Tc-NFC labeling method for the aforementioned parameters was found highly efficient; typically resulting in over 95% binding rate, while less than 5% of the technetium remained unbound (Fig. 2). Reference samples without stannous chloride showed little binding efficiency. In addition NFC did not show any inherent binding affinity towards ^{99m}Tc.

In preparation for the *in vivo* animal experiment, the radiolabel stability was studied for a period of 24 h in both saline and fetal bovine serum (FBS) samples (Fig. 3). ^{99m}Tc-NFC was shown to be stable in FBS during the 24 h period. In contrast, the radioactivity of the labeled NFC in saline at the 24 h time point was reduced to 40.5%. During the first 4 h, the overall radioactivity of ^{99m}Tc-NFC remained at 81.7% and 87.2% for saline and FBS samples, respectively. Therefore it can be expected that the radiolabel will remain stable during the first stages of the SPECT/CT imaging; however some consideration has to be taken into account while examining the 24 h data.

3.2. In vivo imaging, drug release and kinetics models

The location of the NFC hydrogel after injection was investigated with a dual-trace SPECT/CT imaging of ^{123}I-NaI and ^{99m}Tc-NFC. Images confirm the hydrogel position at the injection site in the pelvic region (Fig. 4). In addition, the NFC hydrogel remained intact during the image acquisition. In between the first set of images and the 5 h images, the mice were awake and moving freely

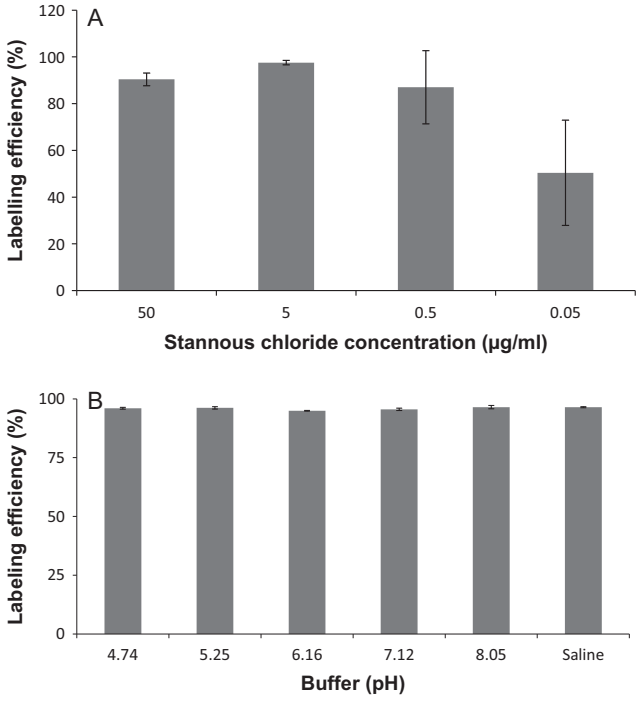

Fig. 1. The effect of the amount of stannous chloride and pH in ^{99m}Tc-NFC radiolabel preparation. (A) No major differences were found between the concentration levels of 50–0.5 μg/ml of stannous chloride. Optimal concentration was found at 5 μg/ml and used in the later phases of this study. (B) The labeling solution pH levels between 4.74 and 8.05 did not show any clear effects in the final radiolabeling efficiency. The labeling solution pH of 7.2 was used in the animal studies.

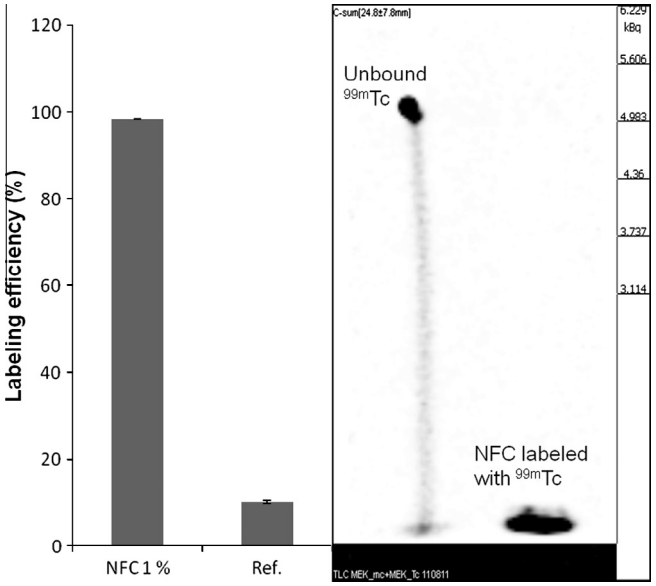

Fig. 2. The labeling efficiency of NFC with ^{99m}Tc-pertechnetate. Typically over 95% binding was observed. Samples that were not treated with stannous chloride showed poor labeling efficiency (Ref.), suggesting that NFC does not have an inherent binding affinity towards the radiolabel in its unoxidized state. With the absence of NFC the free $^{99m}TcO_4^-$ does not remain at the point of application (shown on the SPECT/CT image taken from a TLC sheet). When NFC is introduced with $^{99m}TcO_4^-$, only a small portion of the radiolabel is shown unbound.

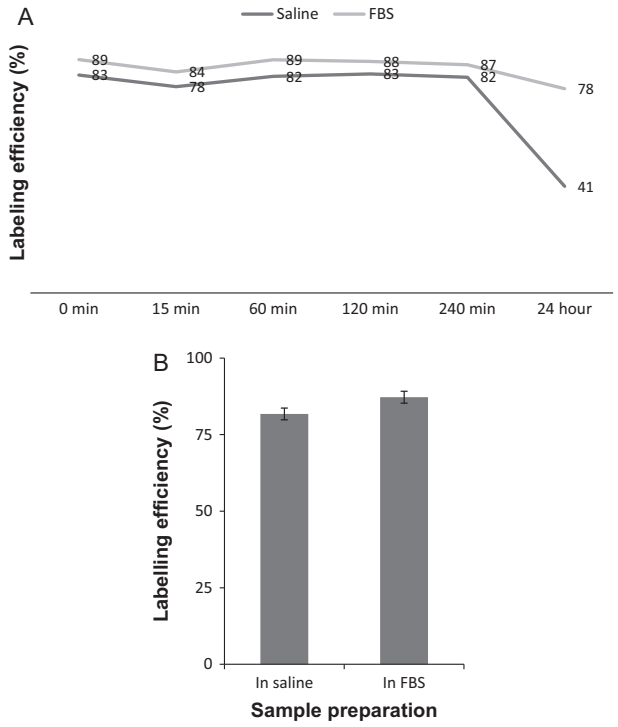

Fig. 3. The stability of the ^{99m}Tc-NFC radiolabel during a 24 h period. (A) The sample prepared in FBS remained relatively stable during the whole experiment; however the sample prepared in saline showed a major decrease of labeling efficiency at the end point of the study. (B) The overall labeling efficiencies suggest that both samples are stable during the first 4 h after sample preparation.

in their habitats. During this time, the hydrogels did not migrate nor disintegrate. Furthermore, the radiolabel showed stability as predicted from the previous radiolabel stability experiment (Fig. 3), and the pertechnetate remained at the injection site bound to the NFC hydrogel. ^{123}I-NaI was mostly distributed into the thyroid glands and stomach, in addition to being excreted to urine. 5 h post injection, no trace of ^{123}I-NaI was found at the injection site.

To explore the use of the NFC hydrogel as a drug release matrix, we selected a small drug (^{123}I-β-CIT) and a large protein drug (^{99m}Tc-HSA) to evaluate the effect of molecule size on the rate of release from the NFC hydrogel. The *in vivo* release and distribution of ^{123}I-β-CIT and ^{99m}Tc-HSA were investigated after injecting the NFC hydrogels imbedded with the study compounds. The study compound and saline solution mixtures were used as controls (injections without the NFC hydrogel).

The differences between the HSA–NFC hydrogel "implants" and saline injections were observed as ^{99m}Tc-HSA expressed a delayed release from the NFC hydrogel and 41% of the injected dose remained within the hydrogel 5 h post injection (Fig. 5a). Linear release was observed in the beginning of the study, and release rates calculated from the early time points (from first to 5 h) resulted in −0.0233 μg/h and −0.0139 μg/h for saline solution and hydrogel injections, respectively. Release of ^{99m}Tc-HSA was steady during the whole study. In addition, a large distribution of ^{99m}Tc-HSA was shown in the subcutaneous tissue surrounding the injection site indicating a very poor absorption of ^{99m}Tc-HSA into the circulatory system (Fig. 5b). Slight activity was detected within the bloodstream, as indicated by the radioactivity in heart and left kidney (Fig. 6). However, the distinctions between the compound itself and its metabolites cannot be made, as it is well known that ^{99m}Tc-HSA does not pass the glomerular filtration under normal renal activity. Slow absorption is probably due to the large protein size and low enzymatic activity within the subcutaneous tissue. It was shown that injections given with NFC hydrogel retained ^{99m}Tc-HSA in a smaller area within or around the hydrogel than saline solution injections (Fig. 5b), therefore ^{99m}Tc-HSA did not freely distribute into the subcutaneous tissue. This might indicate that rate of release from the hydrogel is limiting ^{99m}Tc-HSA absorption.

Heart and the left kidney were selected to estimate the ^{99m}Tc-HSA absorption into the cardiovascular system. No apparent accumulation of ^{99m}Tc-HSA to any other organ was detected. No differences between the saline and hydrogel injections were observed in blood pool activity, i.e. heart (Fig. 6a). However, slight differences were detected in the left kidney of the study animals (Fig. 6b). The amount accumulated in the left kidney during the study period was low in addition to some of the activity might be due to metabolized ^{99m}Tc-HSA. However the differences indicate a slower absorption from the NFC hydrogel injections. Therefore the limited distribution (smaller surface area) might explain the lower absorption rate from the ^{99m}Tc-HSA/NFC.

To better understand the release profile of ^{99m}Tc-HSA from the NFC hydrogel, we performed pharmacokinetic simulation by using the built-in 1-compartmental models of Phoenix® WinNonlin®. We used both deconvolution and Loo–Riegelman models to depict the fraction that is ready to be absorbed from the initial injection site, i.e. the hydrogel. Both models show similar profiles, in addition to most of the dose being ready for absorption at the 24 h time point. Both pharmacokinetic models built for ^{99m}Tc-HSA showed an absorbed fraction of ∼0.43 over 15 min post-injection (Fig. 7). The release was shown as 1st order kinetics. The computational elimination rate constants were 0.108 h^{-1} and 0.209 h^{-1} from the hydrogel and saline solutions, respectively (Supplementary Table 1); therefore showing a 2-fold slower rate of elimination of ^{99m}Tc-HSA from the injection site when given with the hydrogel. It should be noted that the absorbed fraction depicted in the pharmacokinetic models does not describe the absorption that was seen in the SPECT/CT images, but rather the distribution within the subcutaneous tissue. The SPECT/CT images show a clear signal for ^{99m}Tc-HSA at 24 h post-injection.

In contrast to a larger compound, ^{99m}Tc-HSA that showed a slow release from both NFC hydrogel and saline mixture (Fig. 5), the small compound ^{123}I-β-CIT was released rapidly from the NFC injections (Fig. 8). 5 h post-injection ^{123}I-β-CIT had been completely released from the NFC matrix. Slightly slower release was observed with ^{123}I-β-CIT/NFC hydrogels compared to the ^{123}I-β-CIT/saline injections; however the differences were not apparent. A similar effect was observed with ^{123}I-β-CIT than with ^{99m}Tc-HSA, as the NFC hydrogel retains the study compound within itself and a smaller area than with the saline injections. Therefore a better indication for smaller compounds with the use of NFC hydrogels might be local delivery rather than delayed delivery which was observed with the larger compound ^{99m}Tc-HSA.

In summary, the release rate and distribution of ^{99m}Tc-HSA indicated a clear difference between the NFC hydrogels and saline solutions. The NFC hydrogel caused a 2-fold slower rate of elimination of ^{99m}Tc-HSA from the injection site. The release was shown to be steady during the 24 h study period. Poor absorption was observed, as ^{99m}Tc-HSA distributed mostly in the subcutaneous tissue surrounding the injection site if given with saline solution. The SPECT/CT images show that both study compounds ^{123}I-β-CIT and ^{99m}Tc-HSA are more concentrated at the injection site when administered with the NFC hydrogel compared with saline solutions. 24 h post-injection small amounts of ^{123}I-NaI dose were found in the thyroid glands for both saline and NFC hydrogel injections. ^{123}I-β-CIT was mostly distributed into the striatum. Other distribution into specific organs in the periphery was unclear, and no other organs were selected to investigate within this study.

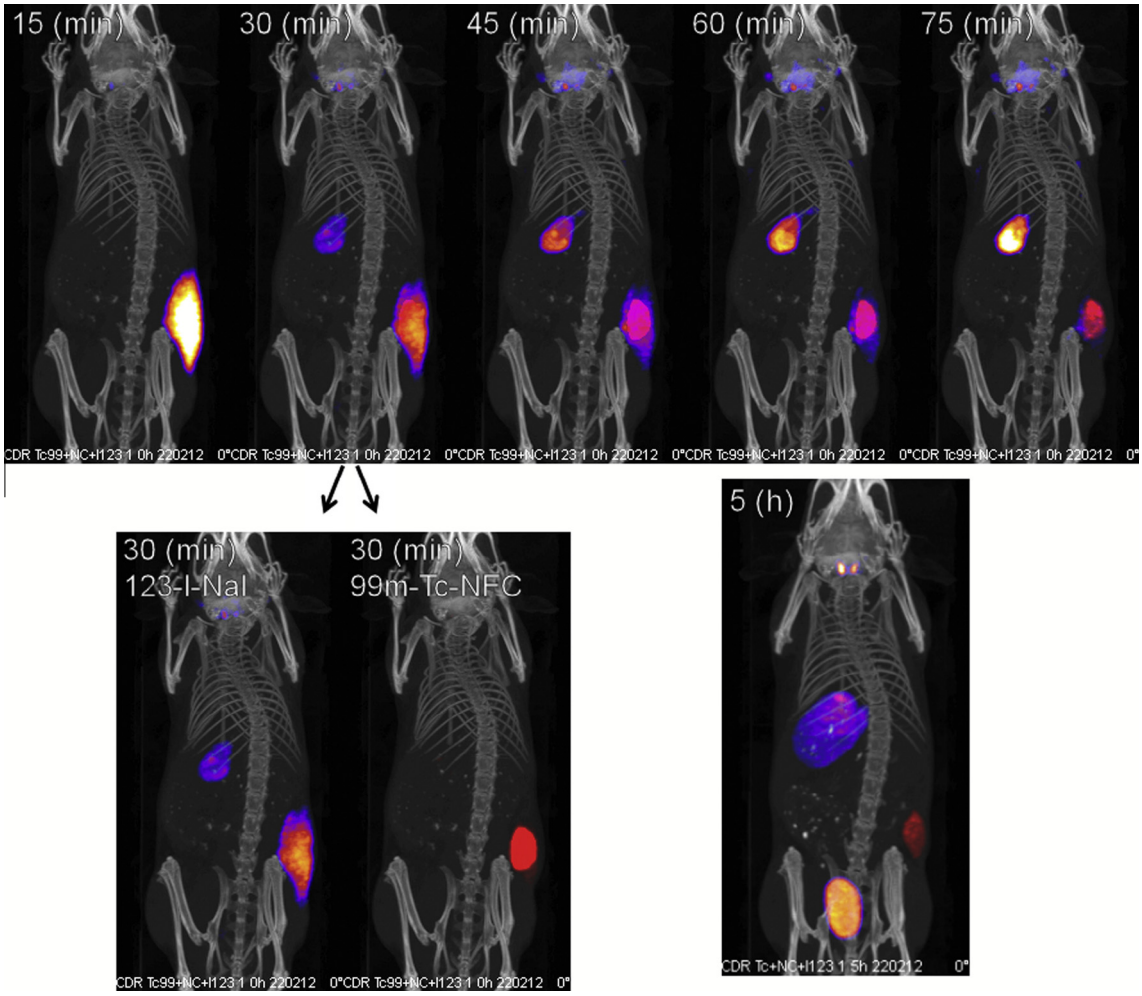

Fig. 4. The release of ^{123}I-NaI from ^{99m}Tc-NFC injections. Above: dual tracing images showing implant (red) placement and test compound release. Below: 30 min image split to visualize both radiotracers separately and the 5 h dual tracing image. ^{99m}Tc-NFC does not seem to disintegrate, migrate or absorb into the bloodstream, although the study animals have been moving freely before the 5 h images. The NFC injections are functioning like drug releasing "implants".

4. Discussion

In this study, the drug release properties of a plant-derived NFC hydrogel, GrowDex®, as an injectable biomaterial were evaluated. NFC samples were imbedded with the labeled study compound for SPECT/CT small-animal imaging, in addition to dual-radionuclide tracing to confirm the *in vivo* localization of the hydrogel. Subcutaneous administration in the pelvic region was selected as the most appropriate and convenient for hydrogel implantation. Injections under the skin can overcome some of the delivery problems related to new biopharmaceutical drugs, such as recombinant human proteins or monoclonal antibodies (Kumar et al., 2006; Muller and Keck, 2004). Additionally, the study compound ^{99m}Tc-HSA would be exposed to the high proteolytic activity in the gut through oral administration. Furthermore, as the native NFC is not naturally degraded in mammals, the subcutaneous site was selected to enable easier later removal of hydrogel implants.

First, we investigated the labeling efficiency of NFC with ^{99m}Tc. The results indicate that after optimization the labeling method showed a high binding rate with less than 5% remaining unbound; therefore achieving a very high binding efficiency. It is possible that the unbound pertechnetate accumulates in the thyroid glands; however the amount (and therefore the signal) remained negligible when compared to ^{123}I-NaI, which is generally known to accumulate heavily into the thyroid. Additionally, ^{99m}Tc was not detected in the thyroid glands in its respective channel in the split images (30 min image in Fig. 4). It is not fully known what the final complex is between cellulose and technetium; however we propose the formation of a chelate complex between NFC and the transition metal technetium that is reduced by stannous chloride, which is a generally used radioactive labeling method (the technetium reduction method). The reduced form Tc^{4+} will form chelate complexes with NFC in the presence of O atoms in the OH groups as it is known that the native NFC is slightly anionic (Kolakovic et al., 2012; Wang et al., 2011). Furthermore it has been shown that cellulose is capable of forming chelates with other transition metals (Kennedy et al., 1974). We propose that the Tc^{4+} aligns itself between the cellulose molecule chains where the natural interchain bonds take place.

The dual-radionuclide tracing SPECT/CT images showed that the NFC implants had remained in their site of implantation during the whole study. The mice have been awake and moving in between acquisitions, which indicate that the NFC hydrogel implants were resisting movement without deforming and did not migrate within the subcutaneous tissue. This suggests that the 0.83% NFC hydrogel is enough to enable fiber rearrangement to revert the shear thinning effect of the extruding force in the needle after administration, which additionally reduces migration of the material within

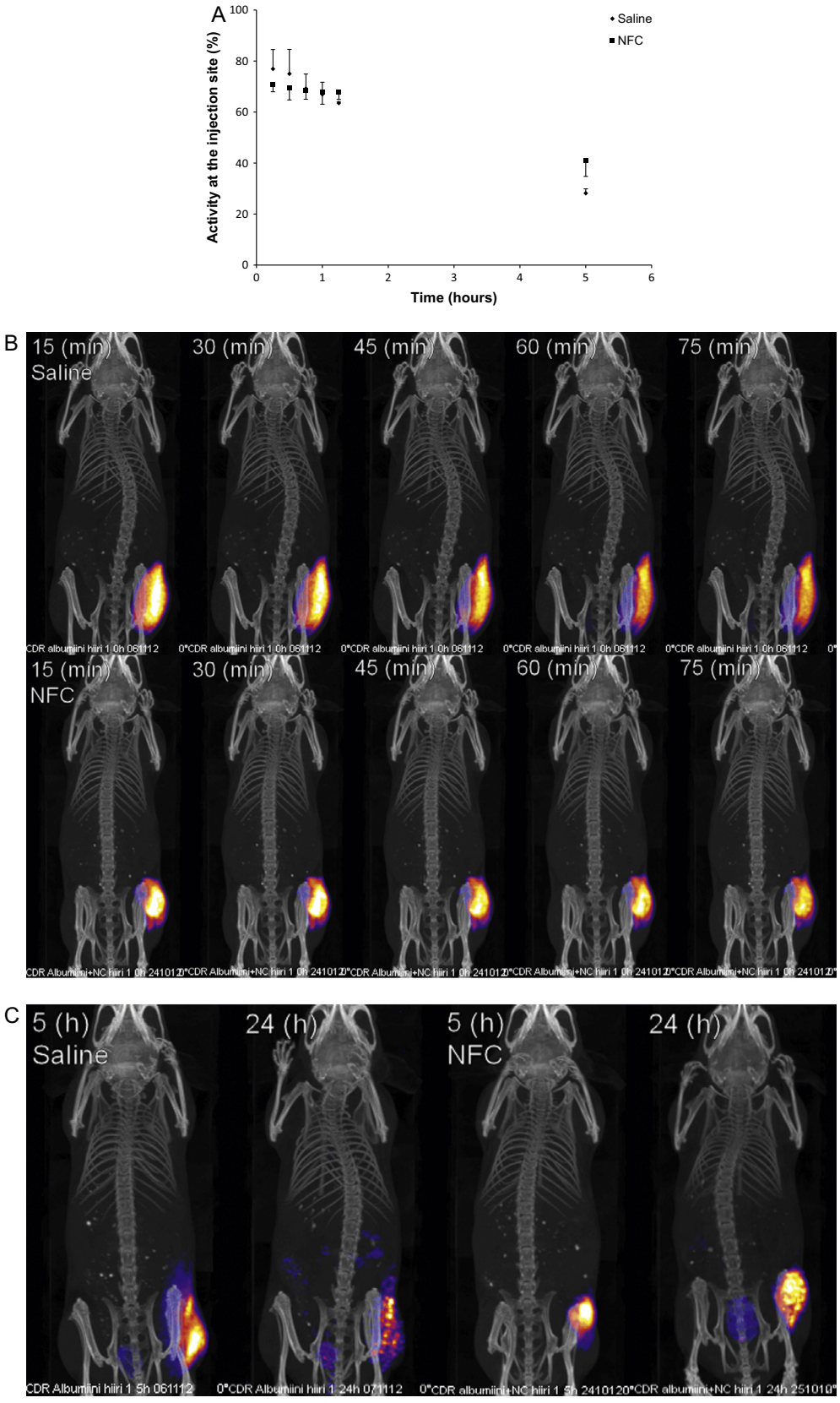

Fig. 5. The release rate of ^{99m}Tc-HSA from saline and NFC injections (% of dose). (A) ^{99m}Tc-HSA showed a slower release profile than the smaller study compounds. In addition, a slower release from the NFC hydrogels in comparison to the saline mixtures was observed. The release profiles for both saline and implant injections were steady. (B) SPECT/CT images of ^{99m}Tc-HSA release from saline (above) and NFC injections (below). NFC hinders the distribution of ^{99m}Tc-HSA within the subcutaneous tissue. In addition absorption is slow from both injections, probably due to the large size of the protein, and low enzymatic activity within the subcutaneous tissue. (C) In the 5 and 24 h SPECT/CT images of ^{99m}Tc-HSA saline (left) and NFC injections (right) ^{99m}Tc-HSA is localized in the NFC implants, and its distribution in the subcutaneous tissue is much lower than in the saline injections. In addition, it was shown that larger amount of ^{99m}Tc-HSA was still present within the hydrogel at 24 h, which indicates a slower rate of release from the NFC hydrogels than from the saline injections.

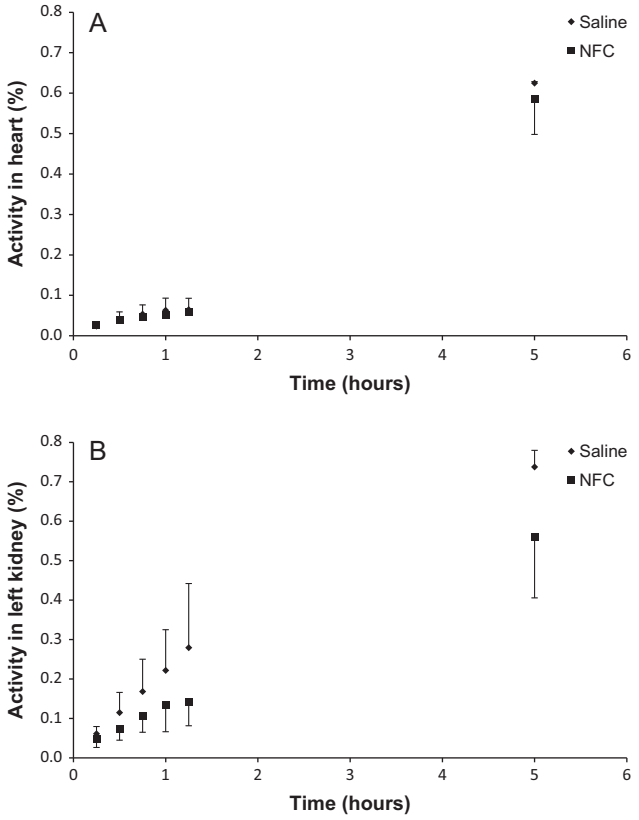

Fig. 6. The blood pool imaging of ^{99m}Tc-HSA. (A) Low activity in the heart suggested poor ^{99m}Tc-HSA absorption from the injection site. No differences between the saline and NFC hydrogel injections were observed. (B) The accumulation of ^{99m}Tc-HSA in the left kidney was low for both saline and NFC hydrogel injections. The activity in the left kidney might be due to metabolized ^{99m}Tc-HSA. However, it also indicates a slower absorption of ^{99m}Tc-HSA from the NFC hydrogels, which according to the SPECT/CT images, is due to NFC hindering the subcutaneous distribution of ^{99m}Tc-HSA.

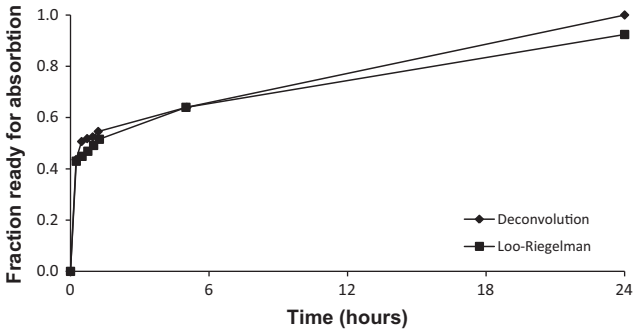

Fig. 7. Pharmacokinetic models showing the estimated fraction ready to be absorbed during the time scale of the study. Deconvolution and Loo–Riegelman models help in estimating the rate of release of ^{99m}Tc-HSA from the hydrogel. Initial release is rapid until the immediate area surrounding the hydrogel is reached, from which after new drug molecules are introduced at a considerably slower rate to the surrounding tissue.

the subcutaneous tissue. Furthermore, the SPECT/CT images indicated that the NFC hydrogels did not degrade or deform as no pertechnetate was observed outside the site of injection, which is supported by the previous studies on cellulose biodurability (Märtson et al., 1999), flexibility, and structural integrity (Pääkkö et al., 2008). As a non-biodegradable material in the mammalian body, NFC could find potential use as a surgical tissue adhesive, space-filling injectable biomaterial for tissue repair, long-term or single-dose local drug delivery, and tissue engineering. However, non-biodegradability is generally not desired. The removal of NFC from easily accessible sites (such as from subcutaneous tissue) through surgical means is fairly simple. In addition, the area could be locally treated with cellulose degrading enzymes to disintegrate the NFC hydrogels yielding mostly glucose as the metabolized product. It has been shown that enzymatic degradation of NFC with cellulase is possible without increasing *in vitro* cytotoxicity (Lou et al., 2014). However, patient acceptance towards injections is generally poor. Therefore NFC hydrogels have potential as long-term or single-dose local delivery systems, especially with compounds of poor bioavailability or where non-invasive routes remain a challenge.

The release and distribution of ^{123}I-β-CIT (a cocaine analogue) from NFC hydrogel implants were evaluated. ^{123}I-β-CIT showed rapid release from the hydrogels, mostly distributing into the striatum and slightly around the hydrogel at the injection site. ^{123}I-β-CIT showed a slightly slower rate of release when imbedded with the hydrogel as opposed to the injections of saline and drug compound solutions. However, due to the rapid release, we determined that ^{123}I-β-CIT does not show an apparent binding affinity to nanofibrillar cellulose itself. In addition, no major differences were found in the distribution of ^{123}I-β-CIT between the NFC/study compound injections and the saline/study compound injections. Therefore it is possible that the release of similar small compounds might not be altered by the NFC matrix. However it seems that the NFC hydrogel retains most of the ^{123}I-β-CIT around itself and does not distribute as easily into the surrounding subcutaneous tissue than with the saline injections. We found it interesting that without affecting much of the release rate of the study compound, ^{123}I-β-CIT is still more localized when administered with NFC.

The release rate of the ^{99m}Tc-HSA was shown much slower than the release rate of the smaller study compound ^{123}I-β-CIT. In addition, a very poor absorption from the injection site into the circulation was observed; furthermore, ^{99m}Tc-HSA distributed heavily into the surrounding subcutaneous tissue. The release rate of ^{99m}Tc-HSA was steady during the whole study period; however, slower release was observed with the NFC hydrogel injections than with the saline injections. This suggests that NFC as an injectable drug releasing biomaterial is indeed more suitable for larger compounds, such as macromolecular protein and peptide drugs. Additionally, protein drugs suffer from delivery problems, which need to be overcome for effective treatment (Jain et al., 2013). As an injectable hydrogel, NFC could solve some of the challenges related to the delivery of biopharmaceuticals.

The pharmacokinetic models that we constructed could be used to further evaluate the release properties of NFC or other biomaterials in conjunction with SPECT/CT imaging. In our study the deconvolution and Loo–Riegelman models described the amount ready to be absorbed, which relates to the release rate of the compound. This could be useful in further analyzing poorly absorbing compounds (such as the HSA in our case), and can be used to complement drug-biomaterial studies when small-animal imaging is in use. This is especially true in situations where poor absorption is the reason for an apparent slow rate of release, which might be an erroneous indication by the SPECT/CT. Therefore, the detected activity at the injection site might not be because of slow rate of release from the biomaterial, but actually due to very poor absorption.

As we proposed earlier, the high biodurability of NFC suggests that as for a non-biodegrading material, it could have a potential use as a long-term drug releasing biomaterial; ideal as an extended release product for chronic diseases. In addition, NFC hydrogels imbedded with therapeutic compounds could find a potential application as a local delivery biomedical device. Topical and subcutaneous conditions could be treated with easily injectable NFC

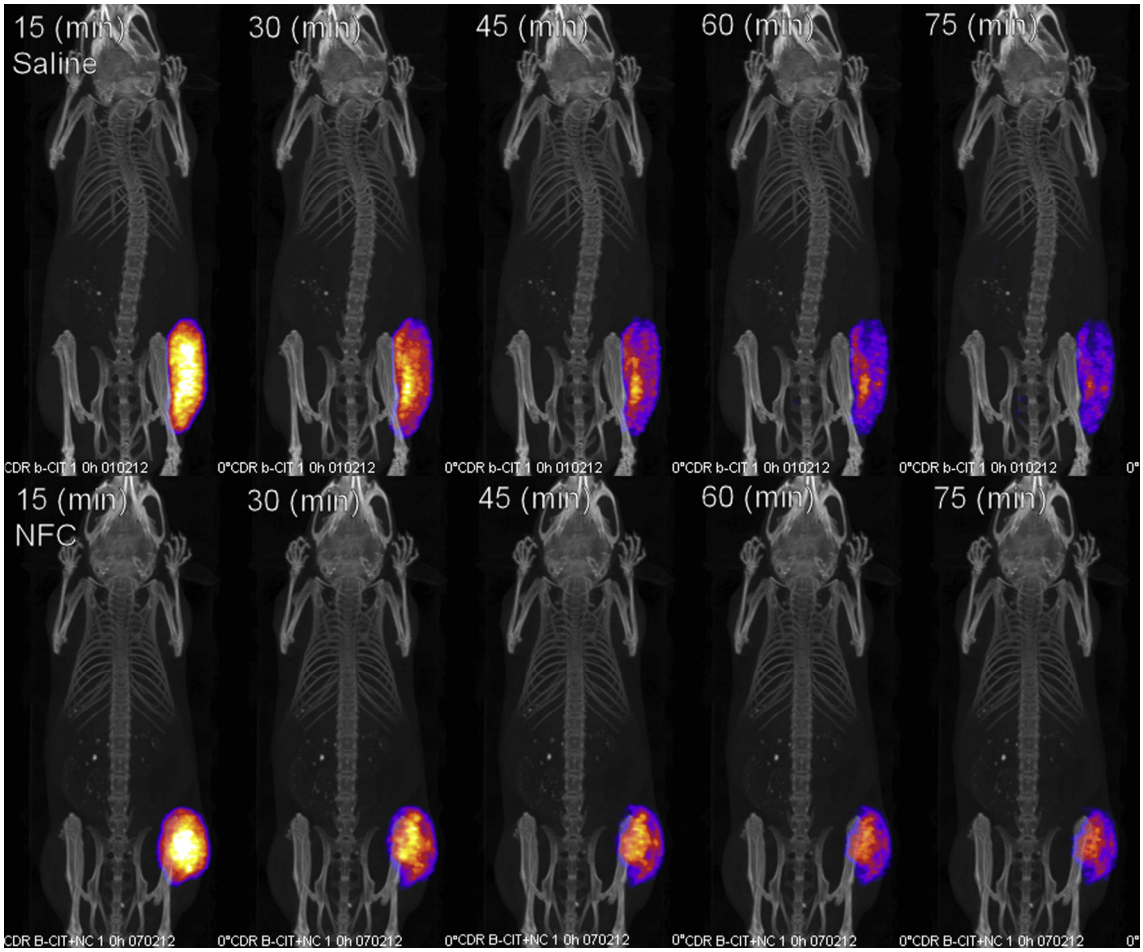

Fig. 8. ^{123}I-β-CIT was shown to be more concentrated at the injection site with NFC injections. Saline injections distributed to a wider area inside the subcutaneous tissue. NFC retains both of the study compounds (^{99m}Tc-HSA and ^{123}I-β-CIT) to a smaller area; however the differences in rate of release/absorption for ^{123}I-β-CIT were small between the injections. This suggests a possible application for local delivery rather than delayed release for smaller compounds used with NFC hydrogels.

hydrogels that can be later enzymatically removed. The steady and continuous release of drug from the hydrogels could be further improved through formulation processes, in addition, nanofibrillar cellulose has not shown cytotoxic properties in previous studies (Vartiainen et al., 2011; Alexandrescu et al., 2013; Pitkänen et al., 2010), which supports the idea of NFC as a potential biomaterial. However, it should be noted that studies considering the safety of plant-derived NFC in humans have not been done and especially with possible long-term exposure, this should be investigated thoroughly.

The possible chemical interactions between proteins and NFC should be investigated individually. NFC contains many hydroxyl groups as well as some carboxyl groups which might interact with the drug compounds imbedded within the matrix; therefore making the predictions of release profiles difficult for different compounds. However, considering the current increase of interest in pharmaceutical research towards the possibilities of macromolecular protein and peptide drugs, NFC might offer an additional method for parenteral delivery, as the effective delivery of protein drugs has been one of the main challenges in pharmaceutical sciences (Kumar et al., 2006). It is likely that the native NFC requires modification to perform more effectively in protein delivery. However cellulose based materials are highly modifiable (Klemm et al., 2011), with which it is possible to improve the properties of NFC in drug release and retaining.

Furthermore, this study did not focus on physical nor chemical properties of the molecules; however the native NFC is known to have a slight negative surface charge (Kolakovic et al., 2012; Wang et al., 2011), thus it can be expected to have some repelling forces between the negatively charged ^{123}I-NaI and ^{99m}Tc-HSA. Indeed, the results indicated that in the dual-radionuclide imaging study, the release of ^{123}I-NaI was more rapid from the hydrogels than from the control saline injections. The chemical properties are more important in smaller scale, thus the repulsion forces by the negative charges are greater than the hindrance of the nanofibrous matrix of the hydrogel itself, which relates to molecular size, a physical factor. ^{99m}Tc-HSA also has a negative charge; however the size of the molecule is considerably larger than ^{123}I-NaI, therefore the physical effect of the NFC matrix in the controlled release is more dominant. Positively charged molecules were not investigated in this study, however considering the effects of the negatively charged molecules (^{123}I-NaI and ^{99m}Tc-HSA); it is likely that a more noticeable sustained release effect would be observed with positively charged molecules.

In addition, during the study on ^{99m}Tc-HSA and hydrogel preparations, it is unlikely but possible that a small amount of the free/unbound pertechnetate from the HSA radiotracer would label the NFC matrix while mixing the ^{99m}Tc-HSA solutions with the biomaterial prior to injection. The labeling for both ^{99m}Tc-HSA and ^{99m}Tc-NFC utilized spontaneous stannous chloride reduction methods;

therefore we believed the labeling mechanism could be the same. In the case of erroneous biomaterial labeling during the study, results would show as a false positive data of slower ^{99m}Tc-HSA release from the biomaterial, as some of the NFC would be labeled to ^{99m}Tc-NFC instead of the ^{99m}Tc-HSA. However, during the radiochemical purity test of the ^{99m}Tc-HSA, the amount of free pertechnetate was observed very low (impurities were found below the allowed 5% indicated by the manufacturer). Therefore, only the free portion of the radiolabel amongst the impurities of the total activity is theoretically able to form bonds with the NFC biomaterial, which would still amount to much less than 5% of the whole activity. This suggests that the ^{99m}Tc-HSA related data obtained in this study is still reliable, as the amount of possible erroneous activity detected from the biomaterial during the image acquisition is considerably lower.

Most injectable biomaterials are prepared in solution, while the gelation is triggered by an external signal, for example phototriggering (Zhang et al., 2002) or salt- and pH-sensitive self-assembly (Collier and Messersmith, 2004). In addition many crosslinking agents are known to be toxic (Speer et al., 1980). Therefore the removal of the potentially toxic crosslinker is required prior hydrogel usage, which may cause additional complications. For NFC, a triggering mechanism is not required, as it is a readily injectable hydrogel in its natural state due to its pseudoplastic and thixotropic properties. This can prove to be advantageous in the use of biomaterials as injectable hydrogels or implants, as there is no additional toxicity or interactions introduced by external activators. Interactions between therapeutic compounds and NFC would still require further investigation; however with the absence of additional activation, processing or crosslinking agent removal, the process is simplified. Additionally, the results indicate that NFC hydrogels could show potential in the delivery of biopharmaceuticals, where parenteral administration could address the delivery problems of protein and peptide drugs. However it is likely that the native NFC requires further modifications for more effective delivery.

5. Conclusions

In this study, we have demonstrated a reliable and efficient method of ^{99m}Tc-NFC labeling. Further research conducted on NFC hydrogels with molecular imaging can be readily performed with this methodology. In addition, our proposed method can help in evaluating the rate of drug release with the use of pharmacokinetic models in conjunction with molecular imaging in drug-biomaterial studies. In the field of non-invasive or minimal invasive research, NFC has potential use as surgical adhesive, space-filling biomaterial in addition to tissue engineering and repair. We performed our study in mind of a potential controlled release or local drug delivery hydrogel that could be easily prepared and readily injected. NFC did not disintegrate or migrate during the study despite the activity of the study animals while awake between image acquisitions. Potential local delivery or long-term controlled release treating chronic diseases, especially in easily accessible areas such as the skin, could be possible with injectable hydrogels. Removal of NFC after treatment can be performed by small surgery or potentially disintegrated into glucose by locally administering cellulose metabolizing enzymes. NFC does not require external activators or crosslinking agents; in addition to it being biocompatible and non-toxic. Further studies to improve hydrogel handling or with specific therapeutic compounds should be performed. However, we have shown the potentiality of wood pulp NFC in the biomedical field, which is complementary to the research already done with bacterial cellulose.

Acknowledgements

This work has been supported by the Finnish Funding Agency for Technology and Innovation, Functional materials program and UPM-Kymmene Corporation, Finland.

Appendix A. Supplementary material

Supplementary data associated with this article can be found, in the online version, at http://dx.doi.org/10.1016/j.ejps.2014.09.013.

References

Alexandrescu, L. et al., 2013. Cytotoxicity test of cellulose nanofibrils-based structures. Cellulose 20 (4), 1765–1775.
Bhattacharya, M. et al., 2012. Nanofibrillar cellulose hydrogel promotes three-dimensional liver cell culture. J. Control. Release 164 (3), 291–298.
Charreau, H., Foresti, M.L., Vazquez, A., 2013. Nanocellulose patents trends: a comprehensive review on patents on cellulose nanocrystals, microfibrillated and bacterial cellulose. Recent Pat. Nanotechnol. 7 (1), 56–80.
Collier, J.H., Messersmith, P.B., 2004. Self-assembling polymer-peptide conjugates: nanostructural tailoring. Adv. Mater. 16 (11), 907–910.
Geckil, H. et al., 2010. Engineering hydrogels as extracellular matrix mimics. Nanomed. (London) 5 (3), 469–484.
Helenius, G. et al., 2006. *In vivo* biocompatibility of bacterial cellulose. J. Biomed. Mater. Res., A 76 (2), 431–438.
Hennink, W.E., van Nostrum, C.F., 2002. Novel crosslinking methods to design hydrogels. Adv. Drug Deliv. Rev. 54 (1), 13–36.
Innala, M. et al., 2013. 3D Culturing and differentiation of SH-SY5Y neuroblastoma cells on bacterial nanocellulose scaffolds. Artif. Cells Nanomed. Biotechnol.
Jain, A. et al., 2013. Peptide and protein delivery using new drug delivery systems. Crit. Rev. Ther. Drug Carrier Syst. 30 (4), 293–329.
Kennedy, J.F. et al., 1974. Active insolubilized antibiotics based on cellulose-metal chelates. Antimicrob. Agents Chemother. 6 (6), 777–782.
Klemm, D. et al., 2011. Nanocelluloses: a new family of nature-based materials. Angew. Chem. Int. Ed. Engl. 50 (24), 5438–5466.
Kolakovic, R. et al., 2012. Nanofibrillar cellulose films for controlled drug delivery. Eur. J. Pharm. Biopharm. 82 (2), 308–315.
Kovacs, T. et al., 2010. An ecotoxicological characterization of nanocrystalline cellulose (NCC). Nanotoxicology 4 (3), 255–270.
Kumar, T.R. et al., 2006. Novel delivery technologies for protein and peptide therapeutics. Curr. Pharm. Biotechnol. 7 (4), 261–276.
Lou, Y.R. et al., 2014. The use of nanofibrillar cellulose hydrogel as a flexible three-dimensional model to culture human pluripotent stem cells. Stem Cells Dev. 23 (4), 380–392.
Lu, T., Li, Y., Chen, T., 2013. Techniques for fabrication and construction of three-dimensional scaffolds for tissue engineering. Int. J. Nanomed. 8, 337–350.
Märtson, M. et al., 1999. Is cellulose sponge degradable or stable as implantation material? An *in vivo* subcutaneous study in the rat. Biomaterials 20 (21), 1989–1995.
Miron-Mendoza, M. et al., 2010. The differential regulation of cell motile activity through matrix stiffness and porosity in three dimensional collagen matrices. Biomaterials 31 (25), 6425–6435.
Moreira, S. et al., 2009. BC nanofibers: in vitro study of genotoxicity and cell proliferation. Toxicol. Lett. 189 (3), 235–241.
Muller, R.H., Keck, C.M., 2004. Challenges and solutions for the delivery of biotech drugs – a review of drug nanocrystal technology and lipid nanoparticles. J. Biotechnol. 113 (1–3), 151–170.
Muller, D. et al., 2013. Neuronal cells' behavior on polypyrrole coated bacterial nanocellulose three-dimensional (3D) scaffolds. J. Biomater. Sci. Polym. Ed. 24 (11), 1368–1377.
Pääkkö, M. et al., 2007. Enzymatic hydrolysis combined with mechanical shearing and high-pressure homogenization for nanoscale cellulose fibrils and strong gels. Biomacromolecules 8 (6), 1934–1941.
Pääkkö, M. et al., 2008. Long and entangled native cellulose I nanofibers allow flexible aerogels and hierarchically porous templates for functionalities. Soft Matter 4, 2492–2499.
Pértile, R.A. et al., 2011. Bacterial cellulose: long-term biocompatibility studies. J. Biomater. Sci. Polym. Ed. 2011, June 28 (epub ahead of print).
Pitkänen, M. et al., 2010. Nanofibrillar cellulose – in vitro study of cytotoxic and genotoxic properties. In: Intl Conf on Nanotechnology for the Forest Products Ind.
Pretzel, D. et al., 2013. A novel in vitro bovine cartilage punch model for assessing the regeneration of focal cartilage defects with biocompatible bacterial nanocellulose. Arthritis Res. Ther. 15 (3), R59.
Roman, M. et al., 2010. Cellulose nanocrystals for drug delivery. In: Polysaccharide Materials: Performance by Design. American Chemical Society, Washington DC, pp. 81–91.
Schade, J.H. et al., 1991. Technetium-99m carboxymethylcellulose: a newly developed fibre marker for gastric emptying studies. Eur. J. Nucl. Med. 18 (6), 380–384.

Slaughter, B.V. et al., 2009. Hydrogels in regenerative medicine. Adv. Mater. 21 (32–33), 3307–3329.
Speer, D.P. et al., 1980. Biological effects of residual glutaraldehyde in glutaraldehyde-tanned collagen biomaterials. J. Biomed. Mater. Res. 14 (6), 753–764.
Van Tomme, S.R. et al., 2008. In situ gelling hydrogels for pharmaceutical and biomedical applications. Int. J. Pharm. 355 (1–2), 1–18.
Vartiainen, J. et al., 2011. Health and environmental safety aspects of friction grinding and spray drying of microfibrillated cellulose. Cellulose 18 (3), 775–786.
Wang, M. et al., 2011. Colloidal ionic assembly between anionic native cellulose nanofibrils and cationic block copolymer micelles into biomimetic nanocomposites. Biomacromolecules 12 (6), 2074–2081.
Zhang, S.J. et al., 2002. Formation of fibrinogen-based hydrogels using phototriggerable diplasmalogen liposomes. Bioconjug. Chem. 13 (3), 640–646.